Journal of Civil Structural Health Monitoring
https://doi.org/10.1007/s13349-025-01004-x

ORIGINAL PAPER

Experimental investigation on story-to-column pounding between RC buildings via shake table tests

Fezayil Sunca[1,2] · Ahmet Can Altunişik[2,3,4] · Ali Kaya[5] · Ali Fuat Genç[7] · Muhammed Cihat Şahin[3] · Algıhan Kaşif Karahasan[6] · Doğa Şen[3]

Received: 30 January 2025 / Accepted: 4 August 2025

Abstract

This study experimentally investigated the effects of story-to-column poundings between adjacent RC buildings through shake table tests. Two scenarios were considered: (i) without pounding and (ii) with story-to-column pounding. The tests were conducted on two 1/2 scaled 2-story RC frames, employing natural ground motion records. The accelerations, displacements, IDRs, and modal parameters of the test specimens were comparatively investigated. The experimental results revealed that pounding significantly influenced structural responses, causing severe shear damage in the columns of the test specimen due to story-to-column collisions. Pounding represented a critical loading condition, inducing abrupt spikes in acceleration responses and resulting in damage. Moreover, pounding caused decreases in displacement responses but led to abrupt increases in base shear forces. This resulted in irregular and asymmetrical hysteresis loops, indicating varying energy distribution in the pounding direction due to repeated impacts. The modal parameters also changed significantly due to the impact, and the changes were observed earlier and more pronounced in the test specimen subjected to pounding.

Keywords Damage · Modal parameters · Pounding · RC building · Shake table test

1 Introduction

In urban areas, it is common to encounter attached buildings that have narrow and null gaps between them. This situation generally arises due to factors such as unplanned urbanization, land conflict/cost, and architectural issues [12, 18]. As a result of this, interaction occurs between adjacent buildings during earthquakes, leading to structural pounding. The earthquake codes and standards suggest numerous principles and guidelines regarding minimum seismic gaps between adjacent buildings, but there is often a tendency to have insufficient gaps between such structures, in practice. Therefore, many urban areas worldwide consist of buildings constructed in proximity or directly adjacent to each other, which could be vulnerable to pounding damage in a

✉ Ahmet Can Altunişik
ahmetcan@ktu.edu.tr

Fezayil Sunca
fezayilsunca@ktu.edu.tr

Ali Kaya
akaya@artvin.edu.tr

Ali Fuat Genç
af.genc@ktu.edu.tr

Muhammed Cihat Şahin
mcssivil@gmail.com

Algıhan Kaşif Karahasan
krhsnalgi@gmail.com

Doğa Şen
senndoga@gmail.com

1 Department of Construction Technologies, Karadeniz Technical University, Trabzon, Turkey

2 Earthquake and Structural Health Monitoring Research Center, Karadeniz Technical University, 61080 Trabzon, Turkey

3 Department of Civil Engineering, Karadeniz Technical University, 61080 Trabzon, Turkey

4 Dynamic Academy Software, Construction Ind. Trade. Co., Ltd. Şti., 61080 Trabzon, Turkey

5 Department of Environmental Engineering, Artvin Çoruh University, 08000 Artvin, Turkey

6 Department of Civil Engineering, Avrasya University, Trabzon, Turkey

7 Of Faculty of Technology, Karadeniz Technical University, Trabzon, Turkey

Published online: 11 August 2025

possible earthquake. Pounding indeed represents a critical load condition during seismic events. It can lead to abrupt spikes in acceleration responses and thus can result in damage to the structural elements of adjacent buildings. During an earthquake, interactions can occur one or multiple times. Pounding-induced damage depends on both the collision force and the recurrence number of strong collisions during an event [1]. Seismic pounding has the potential to cause a wide range of damage, spanning from minor non-structural to severe structural damage. Moreover, these damages can trigger total collapse [24]. Historical events such as the 1985 Mexico City and 1989 Loma Prieta earthquakes have clearly illustrated the destructive consequences of pounding [5, 20, 35]. More recent examples, including the 2011 Lorca, 2015 Gorkha, and 2023 Kahramanmaraş earthquakes, confirm that pounding remains a critical issue leading to severe damage and collapse in urban areas [4, 34, 37].

Existing research has generally considered analytical and numerical modeling approaches aimed at predicting collision behavior. However, although these studies have provided valuable findings, they are often based on idealized boundary conditions or assumptions that simplify contact phenomena. Consequently, experimental studies are needed to accurately assess the collision behavior and damage mechanisms between adjacent buildings under seismic loading. Most of the experimental studies in the literature have various limitations, and most of them used small-scale steel specimens that did not reflect the mass, stiffness, and damage characteristics of existing buildings. Early studies by Filiatrault and Wagner [14], Chau et al. [8], Chau et al. [9], Khatiwada and Chouw [23], El-Khoriby et al. [13], Jankowski et al. [16], Sołtysik et al. [38], and Miari and Jankowski [26] used small-scale steel specimens to examine story-to-story or story-to-column pounding. In addition, some experimental studies have been carried out to reduce the pounding effects using various methods [33, 40]. In addition to these, a few studies have also addressed collision and its destructive effects using large-scale test specimens [11, 17, 29, 36, 39, 41]. However, there are still significant gaps in the research that need to be addressed:

- Lack of experimental studies focusing on pounding between RC buildings, although they are more vulnerable compared to steel structures.
- Experimental studies have mostly focused on story-to-story pounding and few studies have been conducted on story-to-column pounding, which have more destructive effects.
- Lack of large-scale shake table experiments simulating realistic structural behavior.
- A general absence of comparative experimental evaluations between pounding and non-pounding scenarios under the same seismic excitation.

To address these gaps, this study presents a large-scale experimental investigation of the effects of story-to-column pounding between adjacent RC buildings. Two half-scaled two-story RC frames were constructed in laboratory conditions and tested on a unidirectional shake table. In the tests, two scenarios were considered: (i) without pounding case and (ii) with story-to-column pounding case. By focusing on story-to-column pounding, the study aims to fill the existing research gap and contribute to the development of more resilient urban seismic design strategies. The contributions of this experimental study can be listed as follows:

- It presents the limited number of large-scale experimental investigations focusing on story-column pounding in RC buildings.
- It provides a direct comparison of seismic responses between pounding and non-pounding cases experimentally rather than analytically.
- Pounding damages have mostly been studied observationally after past earthquakes. In this study, damages and the effects of collision on structural damages are investigated in detail by vibration tests.
- It provides experimental data to support the recommendations for minimum gap distances in seismic design codes.

2 Experimental campaign

2.1 Design and construction of RC test specimens

The study utilized a two-story full-scale reinforced concrete (RC) building model as a prototype. To represent common urban RC buildings in Turkey, frequently encountered inadequacies including poor concrete quality, inappropriate cross-section dimensions, and lack of lateral reinforcement in structural members and beam-column joints were considered [4]. The design of the frame did not incorporate high-ductility seismic detailing, as the primary aim was to represent common deficiencies observed in existing RC buildings in Turkey. As shown in Fig. 3b, the stirrup spacing in the beam and column elements does not meet the requirements for high ductility detailing as defined by seismic design standards. The detailing was derived from existing RC building stock, rather than from newly designed structures, in order to better represent the seismic performance characteristics of existing building stocks in Turkey. The plan dimensions of the prototype model were 4.20×8.30

m and a total height of 6.00 m. The RC prototype consisted of 15 cm thick floor slabs. The cross-section dimension of the columns and beams was selected as 30×40 cm. It was designed as a bare frame without considering the presence of infill walls. The loads considered consisted of dead loads at 2.00 kN/m^2 and live loads at 2.00 kN/m^2. The concrete had a grade of C14, indicating a characteristic compressive strength of 14 MPa, while the reinforcement employed was of grade S420, characterized by a yield strength of 420 MPa.

In the past, pounding test results reported uncovered that unforeseen torsional reactions might arise because of the collision surfaces between adjacent three-dimensional test specimens not being perfectly parallel during the shake table tests [11]. Therefore, unexpected structural behaviors such as torsion in pounding tests due to problems in the construction of test specimens and test setup can affect the measured responses. In addition, the capacity of the shake table is one of the most important criteria determining the scale factor of the test specimen. The use of three-dimensional specimens necessitates the selection of larger scale factors for capacity reasons. This approach results in much smaller designs compared to the mass and stiffness of real structures. For these reasons, it was decided to use two-dimensional test specimens. To create test specimens, the inner-axis frame of the prototype building was extracted (Fig. 1).

At Karadeniz Technical University's Structural Health Monitoring Laboratory, pounding tests were conducted using a shake table facility as described in this study. The specifications of the shaking table are presented in Table 1. Moreover, its capacity diagram is given in Fig. 2. In pounding tests, half-scaled specimens were used to accommodate the constraints of the shake table and the laboratory conditions. In the scaling process, the artificial mass simulation model was adopted. The material properties of the scaled test specimens and the prototype building were taken to be the same due to the requirements of

Table 1. The specifications of the shaking table used in pounding test

Properties	Capacity
Rigid platform	4 × 4 m
Maximum acceleration	±2 g
Maximum velocity	628 mm/s
Displacement capacity	±400 mm
Effective payload capacity	350 kN
Dynamic lateral load capacity	500 kN

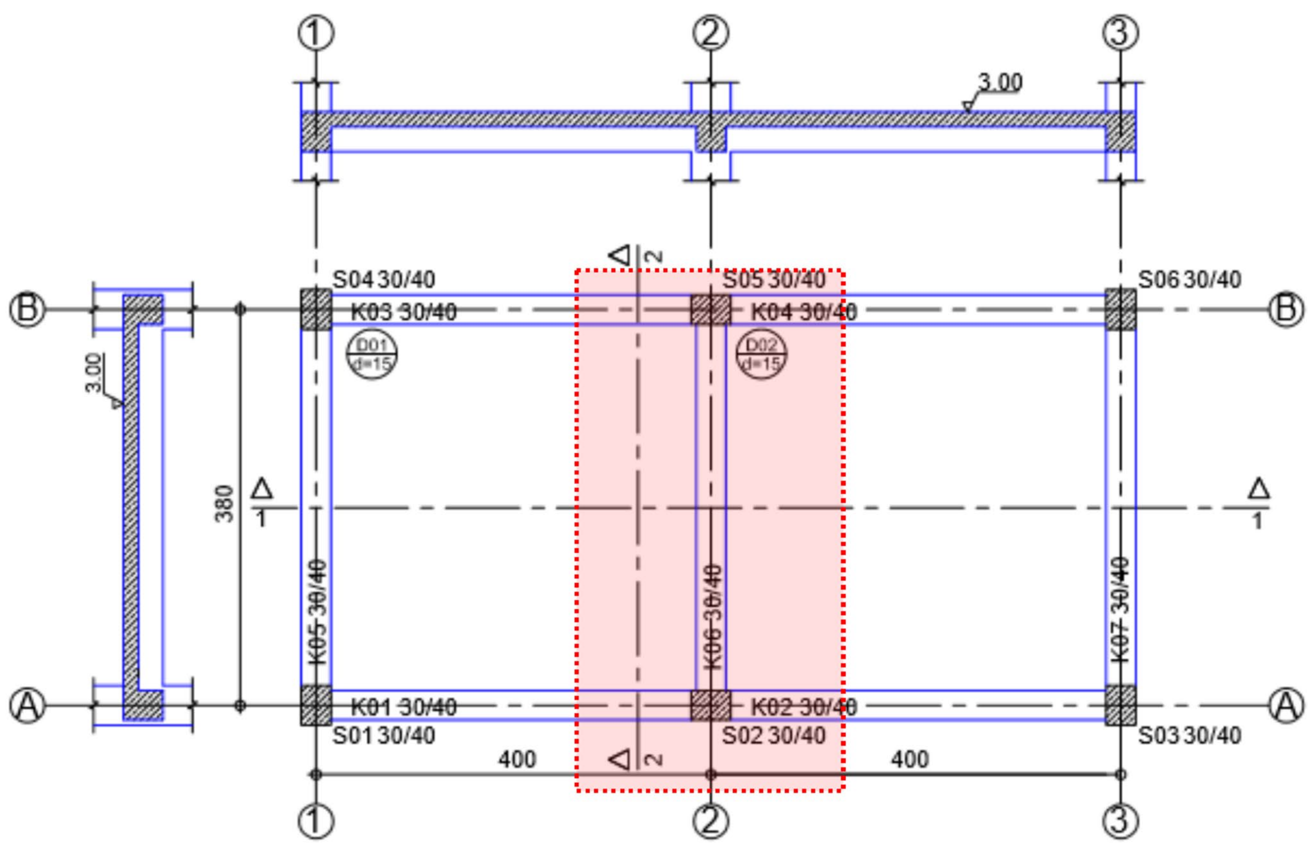

Figure 1. The plan view of the prototype and extracted frame structure (dimensions in cm)

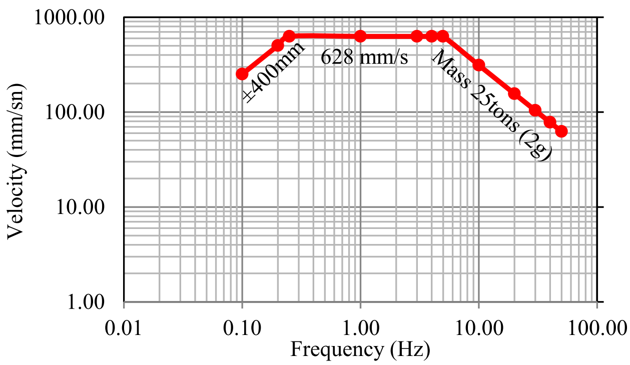

Figure 2. The capacity graph of the shake table with a horizontal force of 500 kN

the adopted scaling procedures. On the other hand, the literature thoroughly outlines the scale factors employed in the artificial mass simulation model, covering various parameters in detail [42]. To ascertain the additional inertial masses to be mounted on the specimens, a mass simulation approach proposed by Quintana-Gallo et al. [32] was employed. The calculations indicated a need for an additional mass of approximately 1.70 tons per story. To simulate these masses, steel plates measuring 250 × 1000 × 16 mm were employed on the slabs at each story level.

Following the scaling process, the single-bay test specimens originally standing at 3.00 m in height were adjusted to 1.50 m. The foundation's dimensions obtained as 0.85 m in width, 2.20 m in length, and 0.40 m in thickness. To fasten up the specimens on the shake table, 16 points on the foundation were equipped with 50 mm diameter holes. Columns and beams had cross-sections measuring 15 × 20 cm. In the columns, longitudinal and transverse bars were configured as 4Φ10 and Φ8/20, respectively. The beams were reinforced with 2Φ10 bars on both the top and bottom zones. The slab had a thickness of 7.50 cm. Holes with a diameter of 50 mm, akin to those in the foundations, were also present in the slabs to affix the additional masses. Figure 3 displays the structural elements' geometric details and reinforcement.

The construction of the specimens progressed in three stages, involving separate construction phases for the foundation and slabs. During each stage, 6 cube samples, 6 cylinder samples (10 × 20 cm), and 6 cylinder samples (15 × 30 cm) were collected to assess concrete strengths, stress–strain curves, and concrete tensile strengths. Material tests yielded average cylinder compressive and tensile strength values for concrete at 14.53 MPa and 1.44 MPa, respectively. In addition, to determine the yield strengths of the reinforcements, laboratory tests were conducted using nine samples. The average yield strengths were found to be 480 MPa for Φ8 bars, 477 MPa for Φ10 bars, and 463 MPa for Φ12 bars.

2.2 Configuration of the test setup

The general view of the test specimens and experimental setup designed specifically for the pounding tests is given in Fig. 4. The alignment of the test specimens was meticulously adjusted to match the shaking direction. In order to counteract sliding or rocking motions of the RC frames, an appropriate connection was established between the foundations and the rigid platform. This was achieved using M20 steel rods at 16 different points in conjunction with steel box-section beams. Following the adopted simulation procedure, 1.70 tons of additional masses were allocated to each floor. To simulate these masses, steel plates measuring 250 ×1000 × 16 mm were employed on the slabs at each story level, fastened using 8 M14 rods (Fig. 4b). During the experiments, an array of 8 roller bearings was employed specifically to inhibit any out-of-plane movements of the RC frame (Fig. 4c). This system allowed the precise positioning of the bearings at designated locations on the specimens.

Most of the experimental studies mentioned in the literature review have examined the collision effects, taking into account buildings with different dynamic characteristics (cases where one building is more flexible or rigid than another). Indeed, performing simultaneous evaluations and measurements of structural responses from two test specimens during shake table experiments is a highly complex task. In addition, connecting two test specimens to the shaking table simultaneously and the additional masses imposed by simulation requirements have exceeded the capacity, necessitating the use of much smaller scale factors. To overcome this situation, a rigid collision wall was constructed using HE200A profiles to simulate the behavior of a rigid building (Fig. 4d). There were studies in the literature that have adopted such an approach. In the literature, there are pounding tests conducted adopting this kind of approach [22]. The rigid collision wall was 4.50 m in height and had a double row of holes spaced 10.0 cm apart on its front face. Through these holes, the RC collision elements could be positioned at the desired elevations and gap distances, enabling the examination of the column–slab collision. The adjustable RC collision elements were fabricated to establish the surface between the specimens and the rigid collision wall and to accurately regulate the gap distances (Fig. 4e). The RC collision elements consisted of the following components: (i) one RC block, (ii) 4 M18×300 steel rods, (iii) 6 M20 × 300 steel rods, (iv) a steel plate (350 × 250 × 20 mm) having 20 mm threaded holes at 6 different points, (v) two steel plates (350 × 50 × 20 mm) having 20 mm holes at 2 different points.

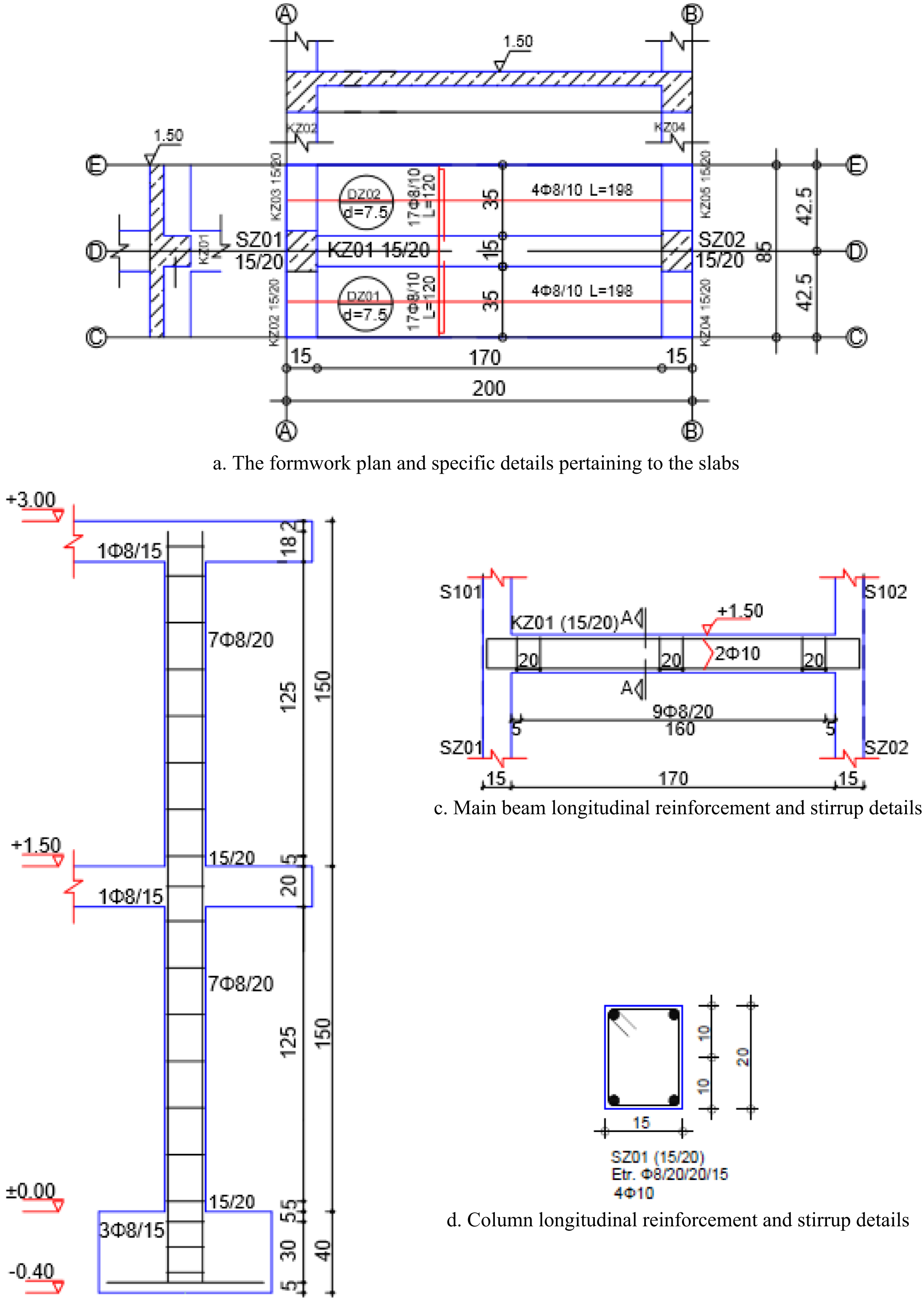

a. The formwork plan and specific details pertaining to the slabs

b. Elevation view of column

c. Main beam longitudinal reinforcement and stirrup details

d. Column longitudinal reinforcement and stirrup details

Figure 3. The test specimens' geometric configuration and reinforcement details (dimensions in cm)

a. The general view of test setup

b. Additional masses on the slabs

c. The roller-bearings to prevent out-of-plane motion

d. The rigid collision wall

e. RC collision elements

Figure 4. Experimental setup

In column–slab pounding scenarios, impacts may occur at any location along the column effective length. The main research issue in this type of collision is the development of a shear-critical condition due to the collision forces in the column where the interaction occurs. If the interaction occurs at the mid-height of the column effective length, equal bending moments develop at both ends of the column, resulting in flexural-critical regions at both the top and bottom ends. In this case, the shear force induced by the impact is also equally distributed between both ends of the column. Conversely, collisions occurring in a region other than the mid-height of the column can create critical conditions in terms of bending in the long part of the column and shear in the short part of the column [19]. In previous studies, to intentionally create shear-critical column regions under column–slab pounding, impact locations have been assumed to occur at 2/3 of the column height [19, 25]. Therefore, collision elements were placed on the rigid wall in a manner that the interaction occurs at 2/3 of the interaction story heights during shake table tests. During the pounding tests, a gap of 5.0 mm was considered between the RC collision elements and the test specimens.

2.3 Test instrumentations

To investigate story-to-column pounding via shake table tests, two half-scaled two-story RC frames were constructed in laboratory conditions. These specimens were instrumented to acquire information about component and global system response and to determine the effects of pounding on these responses. In shake table tests, five uniaxial and three triaxial accelerometers were utilized. To monitor the conformity between the applied and measured responses from the shake table, a uniaxial accelerometer was placed on the rigid platform of the shake table. Three uniaxial accelerometers were installed to track in-plane acceleration responses at the foundation and story levels. Furthermore, the role of roller bearings in preventing out-of-plane motion was investigated using a uniaxial accelerometer placed on the roof level of test specimens. Pounding indeed represents a critical load condition during seismic events. It led to abrupt spikes in acceleration responses and thus resulted in damage to the structural elements of adjacent buildings. Therefore, capturing sudden peaks in acceleration responses during the pounding tests was crucial. To this aim, triaxial accelerometers with a measurement capacity of ±40.00 g and a sampling rate of up to 4.00 kHz were utilized. These accelerometers were placed near the collision zones of the specimens and the rigid wall. To monitor the displacement responses of the shaking table, foundations, and floors, four linear potentiometric displacement transducers (LPDTs) were used. In addition, two LPDTs were set up to measure the relative displacements between the test specimens and the rigid collision wall.

Before and after each shake table test, the frequency, modal shape, and damping ratio were experimentally determined using the ambient vibration testing (AVT) method. This was carried out to comprehensively examine the pounding effects on modal parameters and consequently on damages. During vibration tests, one of the crucial aspects to consider is the type of accelerometer chosen based on the structure's type and frequency range. In this study, eight uniaxial accelerometers of type B&K 4507 B 005 were utilized. In addition, the weight of the accelerometer should be negligible compared to the weight of the structure. The selected accelerometers weigh 4.80 g, which

Table 2. Instrumentation layouts

No	ID	Model	Direction	Capacity	Location
1	Acc-1	SENSEBOX7001	In-plane	±2.0 g	Shake table
2	Acc-2				Foundation of specimen
3	Acc-3				1st floor level of specimen
4	Acc-4				2nd floor level of specimen
5	Acc-5		Out-of-plane		2nd floor level of specimen
6	Acc-6	G-LINK200	In and out-of-plane	±40.0 g	Interaction region at 1st floor level of specimen
7	Acc-7				Interaction region at 2nd floor level of specimen
8	Acc-8				Interaction region at 2nd floor level of collision w.
9	LPDT-1	RTL-400	In-plane	±200 mm	Shake table
10	LPDT-2				Foundation of specimen
11	LPDT-3				1st floor level of specimen
12	LPDT-4				Between specimen and collision wall
13	LPDT-5				2nd floor level of specimen
14	LPDT-6				Between specimen and collision wall
15	Acc for AVTs	B&K 4507 B 005	In-plane	±7.0 g	16 distinct location (joints, collision region, etc.)

is negligible compared to the weight of test specimens. These accelerometers were positioned at potential plastic hinge regions (0.5 h) and the middle of each column and at column-beam joints. Thus, vibration measurements were taken from a total of 16 different points. Table 2 reports the positions, capacities, and models of the instruments used in shake table tests and AVT. Figure 5 summarizes the layout of the measurement equipment.

2.4 Test procedure

Within the scope of the study, two RC test specimens were considered. First, the scenario without pounding effects was examined, and a reference data set was established. In this experiment, a 40 cm gap was left between the collision wall and the RC test specimen, ensuring no interaction occurred between them. In the second case, shake table

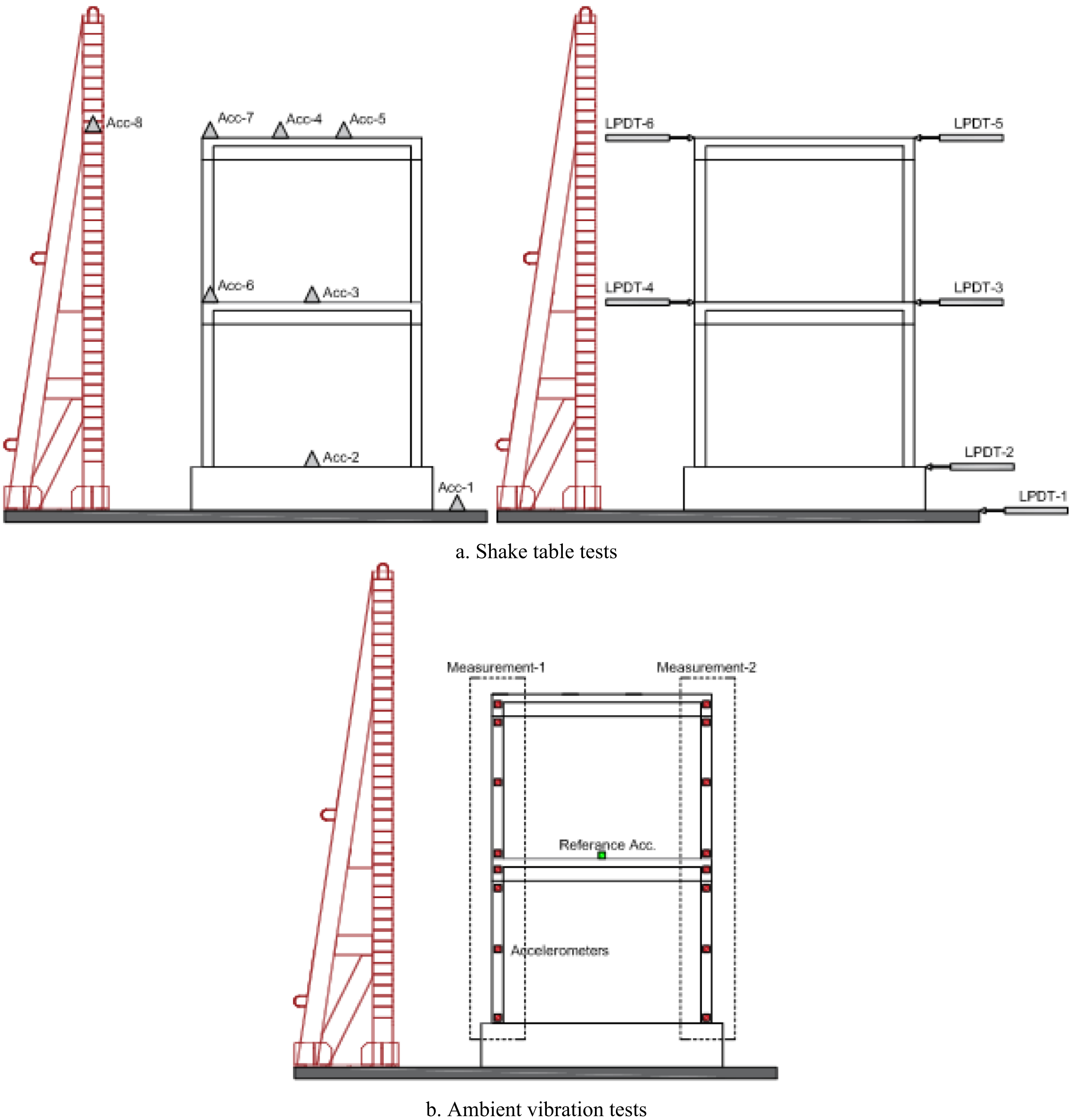

Figure 5. Layout of measurement equipment used in shaking table and ambient vibration tests

tests were conducted to investigate the effects of slab-column poundings. In this case, a 0.5 cm gap was considered between the collision wall and the RC test specimen.

The study utilized two natural acceleration records for shake table tests. The first was the EW component of the 1992 Erzincan earthquake, captured at the Erzincan station, with parameters of PGA = 0.50 g, PGV = 78.16 m/s, and PGD = 28.04 cm. The second was the 090 component of the 2004 Parkfield earthquake, recorded at the Parkfield-Fault Zone 1 station, with parameters of PGA = 0.60 g, PGV = 63.77 m/s, and PGD = 8.46 cm. The records were sourced from the PEER Strong Motion Database [30]. To meet the simulation requirements, the time steps of the records were adjusted using a scale factor of $1/\sqrt{2}$, while the acceleration amplitudes of both the original and scaled records remained unchanged. The acceleration-time graphs of the original and scaled records were presented comparatively in Fig. 6.

Incremental shake table tests were performed by increasing ground motion intensities, measured using PGA values. The 1992 Erzincan earthquake was applied at 25%, 50%, 75%, and 100% intensity levels, while the 2004 Parkfield earthquake was applied at 100% to further assess damage. Table 3 summarizes the loading procedure considered during dynamic tests.

3 Experimental findings and analysis of pounding effects

The discussion highlights how earthquake-induced collisions between adjacent buildings influence observed damage patterns. In addition, this section evaluates the experimental findings from the pounding tests, focusing on parameters such as floor accelerations, displacements, inter-story drift ratios (IDR), and modal parameters.

3.1 Damage patterns and progression

This subsection briefed the damage patterns observed during the shake table experiments, highlighting the effects of pounding on structural components and the progression of damage under varying ground motion intensities.

In the first test specimen, where collision effects were not considered, no visible cracks were observed after the ERZ25. The initial flexure cracks appeared following the ERZ50, which had a PGA of 0.25 g. These cracks were located at the upper ends of the columns on both floors, with widths smaller than 0.10 mm. Furthermore, diagonal cracks appeared in the in-plane beam on the second floor. After the third shake table test, conducted with the ERZ75 ground motion, the cracks at the upper ends of the columns and the joint regions propagated, though both existing and new cracks remained thinner than 0.10 mm. Following the ERZ100, cracks developed at the top ends of the columns, extending across all four faces of the section. In addition, new cracks were observed at the joints, and diagonal cracks appeared in all in-plane beams. Tests performed with the PARKF100 (PGA = 0.60 g) further intensified the damage. The width of existing cracks at the upper column ends increased significantly. Severe damage, including concrete spalling, was observed at the upper ends of the lower floor columns. Cracks also appeared at the lower ends of the columns, about 10.00 cm above the foundation surface. Separation at the interface between the foundation and columns was

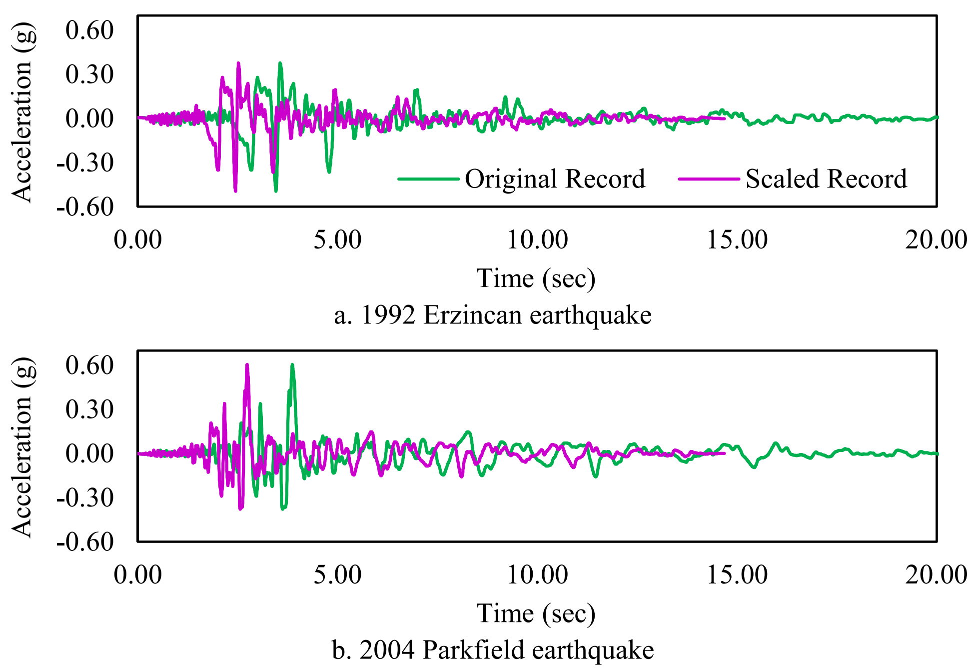

Figure 6. The acceleration-time graphs for the original and scaled records

Table 3. Loading procedure considered during shake table tests

Earthquake	Intensity levels (%)	Code	PGA (g)
1992 Erzincan	25	ERZ25	0.125
	50	ERZ50	0.250
	75	ERZ75	0.375
	100	ERZ100	0.500
2004 Parkfield	100	PARKF100	0.600

particularly pronounced. The crack distribution obtained at the end of this test is presented in Fig. 7.

In the second case, shake table tests were conducted to investigate the effects of slab–column poundings. In the experiments, two-dimensional RC frame specimens were used. As a result, the contact surface was smaller compared to buildings, meaning that the impact energy during interaction was transferred over a relatively limited area. This may lead to more severe localized damage. However, it should also be noted that due to the two-dimensional test specimens, their overall mass was significantly lower than that of existing buildings, and thus, the resulting impact energy was also considerably smaller. In this case, no crack formation was observed after the ERZ25, similar to the first experiment, while damage was recorded following the ERZ50. After the third shake table test conducted with the ERZ75, cracks were detected in the collision region of the second-floor column where pounding occurred. These cracks, oriented perpendicular to the column axis, were narrower than 0.10 mm. In addition, during the interaction between the RC collision element and the column, crushing of the surface

a. Cracks at the top ends of the columns

b. Damage at the joints

c. Diagonal cracks in the in plane-beam

d. Bottom ends of the columns

Figure 7. The damage distribution observed in the scenario without pounding effects

concrete was observed in the second-floor column. Following the ERZ100, shear cracks at an angle of approximately 45° developed in the second-floor column affected by the pounding. These cracks were marked on all surfaces of the column (parallel to the collision direction) and had widths less than 0.10 mm. In low-rise to mid-rise buildings, pounding typically occurs at the top floor. However, in high-rise structures where higher mode effects are significant, pounding may also occur at intermediate floors. Chau et al. [10] stated that if the high-mode response of either or both of the colliding buildings is excited, interaction can also occur at the middle levels of the buildings. In the present study, due to the two-story test specimens, the impact occurred at the second-floor level. Since the specimen approached the collision element at an angle during seismic excitation, the contact occurred between the upper portion of the RC collision element and the column. Therefore, shear damage in the column initiated just above this region (Fig. 8). Tests conducted with the PARKF100 resulted in a significant increase in the width of existing shear cracks in the impacted column. In addition, new shear damage due to pounding was observed, and the progression of cracks at the upper ends of the other columns was also recorded. Due to the interaction occurring between the slab and the column, this type of collision exhibits more destructive effects compared to other collision types. Columns subjected to such collisions are particularly exposed to extremely high shear forces. Past earthquakes have demonstrated that even when these columns comply with regulatory requirements, significant damage can occur due to the increased shear forces resulting from the magnitude of the collision forces during the interaction.

In this study, the RC frames were intentionally detailed with insufficient transverse reinforcement to reflect common deficiencies observed in existing urban buildings in Turkey. The design did not include proper shear detailing in the load-bearing elements or their joints, and no assumptions were made regarding compliance with modern seismic codes. Instead, it was assumed that shear resistance would primarily be provided by the inherent shear strength of the concrete. This approach aimed to realistically represent the structural vulnerabilities of typical existing buildings under seismic impact conditions. These findings revealed that under such impact scenarios, the shear capacity of concrete is inadequate to accommodate the significantly increased shear forces due to impact, especially where detailing is inadequate. On the other hand, previous earthquake investigations have shown that even RC buildings designed in accordance with modern seismic codes can experience significant shear damage due to pounding effects. In particular, when column-story pounding occurs during strong ground motions, the resulting impact forces may exceed the shear capacity provided by code-conforming detailing, leading to shear damage, concrete spalling, or even local failure. These findings highlight the critical role of impact-induced shear

Figure 8. Shear damage observed in the second-floor column due to pounding

demands, which are often underestimated in conventional seismic design approaches.

3.2 Floor accelerations

Pounding indeed represents a critical load condition during seismic events. It led to abrupt spikes in acceleration responses and thus results in damage to the structural elements of adjacent buildings. Therefore, capturing sudden peaks in acceleration responses during the pounding tests was crucial. To this aim, triaxial accelerometers with a measurement capacity of ±40 g and a sampling rate of up to 4.00 kHz were utilized. To better illustrate the abrupt spikes in accelerations caused by collisions, the 2nd floor accelerations recorded during the ERZ100 and PARKF100 ground motions are presented comparatively in Fig. 9.

The increases in floor accelerations caused by poundings rose proportionally with the intensity of the ground motion. This effect was even more pronounced at the 2nd floor level. The increases in peak accelerations caused by pounding, determined based on the instrumental data from the first test specimen (without pounding case), are presented in Fig. 10. The pounding-induced increases in peak acceleration values obtained at the 1st and 2nd floors were calculated as 1.89–5.59% for the ERZ25, 25.12–58.23% for the ERZ50, 42.72–39.34% for the ERZ75, 66.82–105.14% for the ERZ100, and 43.57–135.57% for the PARKF100.

Floor acceleration is a key parameter used in the identification of the dynamic forces applied to structural components. Past experimental investigations have related this to the base shear forces, calculated as the sum of the products of floor accelerations and their corresponding floor masses [2, 21, 27]. Therefore, the pounding-induced increases in acceleration responses also resulted in critical fluctuations in base shear forces. The increases in base shear forces caused by pounding, determined based on the instrumental data from the without pounding case, are presented in Fig. 11. These increases were calculated as 33.80% for the ERZ50, 86.26% for the ERZ75, 118.70% for the ERZ100, and 100.33% for the PARKF100. This situation clearly showed that considering pounding effects during the design phase is crucial, as insufficient gap distances between buildings can lead to severe damage or even total collapse during earthquakes. On the other hand, non-structural elements sensitive to acceleration are particularly vulnerable to inertial forces caused by pounding-induced peaks in floor accelerations, and this highlights the critical importance of addressing pounding effects in structures housing sensitive equipment.

In the test setup, RC frames and a rigid steel frame were used to focus on the behavior of the specimen under pounding. If a real RC moment frame with its own deformation and damage capacity had been used instead, this could have caused some changes in the structural responses and local damage patterns. However, in previous studies on pounding behavior, it is common to model one building as flexible and the other as rigid. Even if two RC specimens had been used in the experimental setup, it is evident that the more flexible structure would be more affected by the pounding. On the other hand, even in the case of pounding between two RC frames, the overall trend of increased story shear forces, similar to that shown in Fig. 11, is expected to remain. Therefore, although the exact structural response may differ, the main conclusion that pounding increases story shear demands would still be valid in a real structural context.

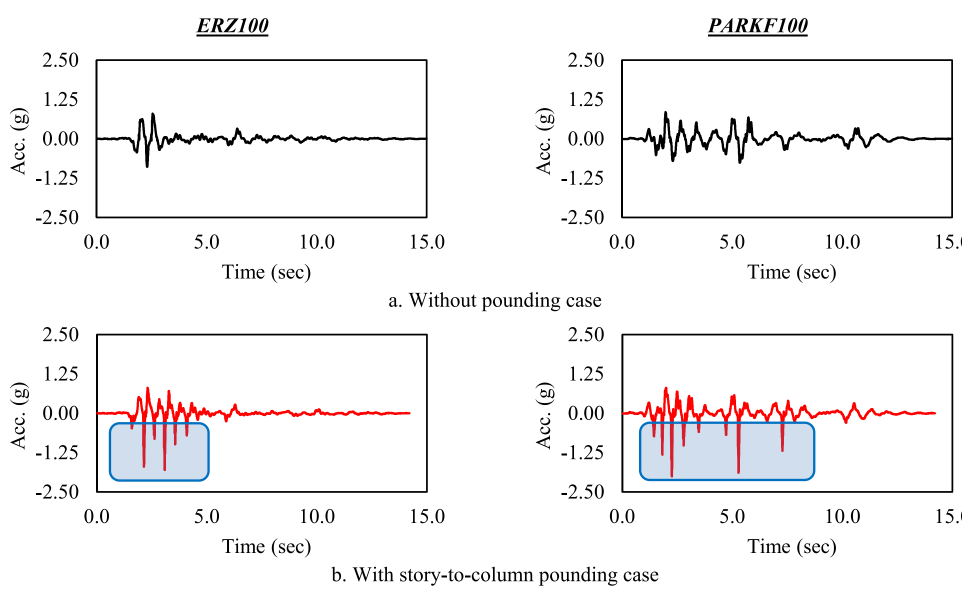

Figure 9. The sudden spikes in floor accelerations caused by story-to-column pounding

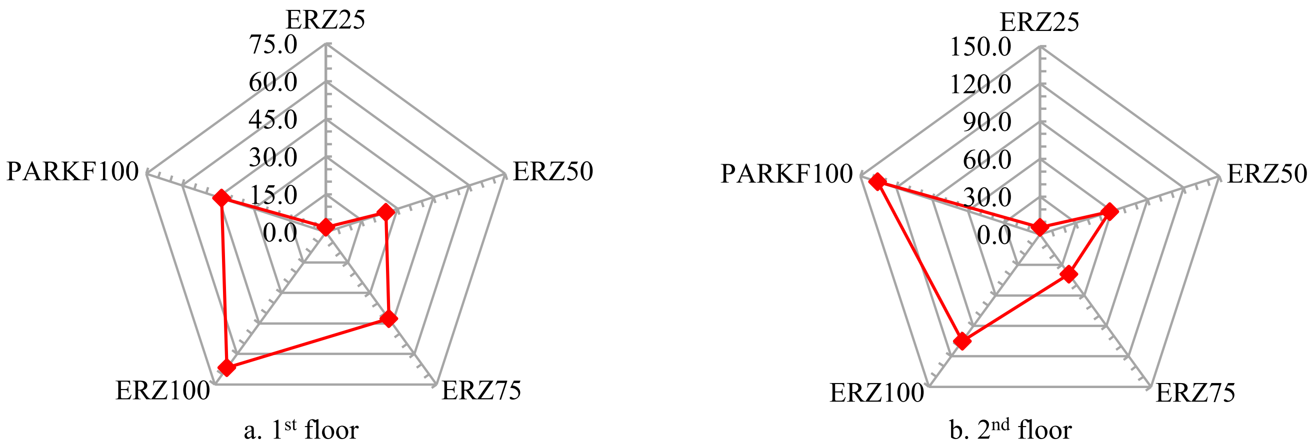

Figure 10. The story-to-column pounding-induced increases in peak floor accelerations

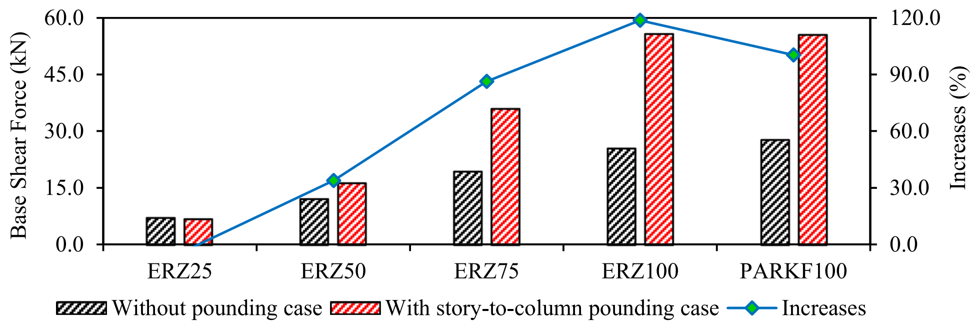

Figure 11. The pounding-induced increases in base shear forces

3.3 Displacements and IDRs

The collision can lead to altered displacement demands in the adjacent structures. Typically, a reduction in displacement responses is expected in the direction of pounding. However, in the direction without interaction, increased displacement demands may occur due to energy transfer between buildings during the pounding. In this study, pounding generally resulted in significant reductions in their displacement responses of test specimens, as observed in the shake table experiments conducted (Fig. 12). However, past studies indicated that displacement responses in the non-pounding (free) direction may increase depending on the energy transferred during the collision [7, 39].

As clearly observed in Fig. 12, the displacement responses in the free direction reached similar amplitudes for both test specimens. However, in the pounding direction, the displacement responses showed a significant decreasing trend due to the interaction between the test specimen and the collision wall. This effect became notably evident as the intensity of the ground motion increased. The changes in maximum displacements caused by pounding, determined based on the instrumental data from the first test specimen (without pounding case), are presented in Fig. 13. For the pounding direction, the pounding-induced changes in maximum displacement values obtained at the 1st and 2nd floors were calculated as 9.27–12.65% for the ERZ25, 35.52–31.85% for the ERZ50, 54.61–66.10% for the ERZ75, 43.90–54.62% for the ERZ100, and 74.45–67.01% for the PARKF100. For the free direction, these changes reached 24.22% for the ERZ25, 5.03% for the ERZ50, 20.31% for the ERZ75, 38.59% for the ERZ100, and 16.11% for the PARKF100.

A comparative analysis of IDRs is an effective approach to evaluate changes in structural behavior under collision effects. Accordingly, Fig. 14 presents the IDRs obtained from the RC test specimens. The interaction between the RC test specimen and the collision wall reduced the IDRs in both the pounding and free directions. In the pounding direction, this reduction reached 74.4% on the first floor and 76.2% on the second floor, while in the free direction, it reached 38.6% and 37.4%, respectively.

A comparison of IDRs can lead to the idea that the pounding-induced decreases in maximum displacements might give the impression of potential benefits to structural behavior. However, the sudden acceleration spikes and the abrupt limitation of motion of the structures ultimately cause significant damage and detrimental effects. To provide a better understanding of this situation, the hysteretic responses of test specimens obtained under ERZ100 and PARKF100 are comparatively presented in Fig. 15. In the

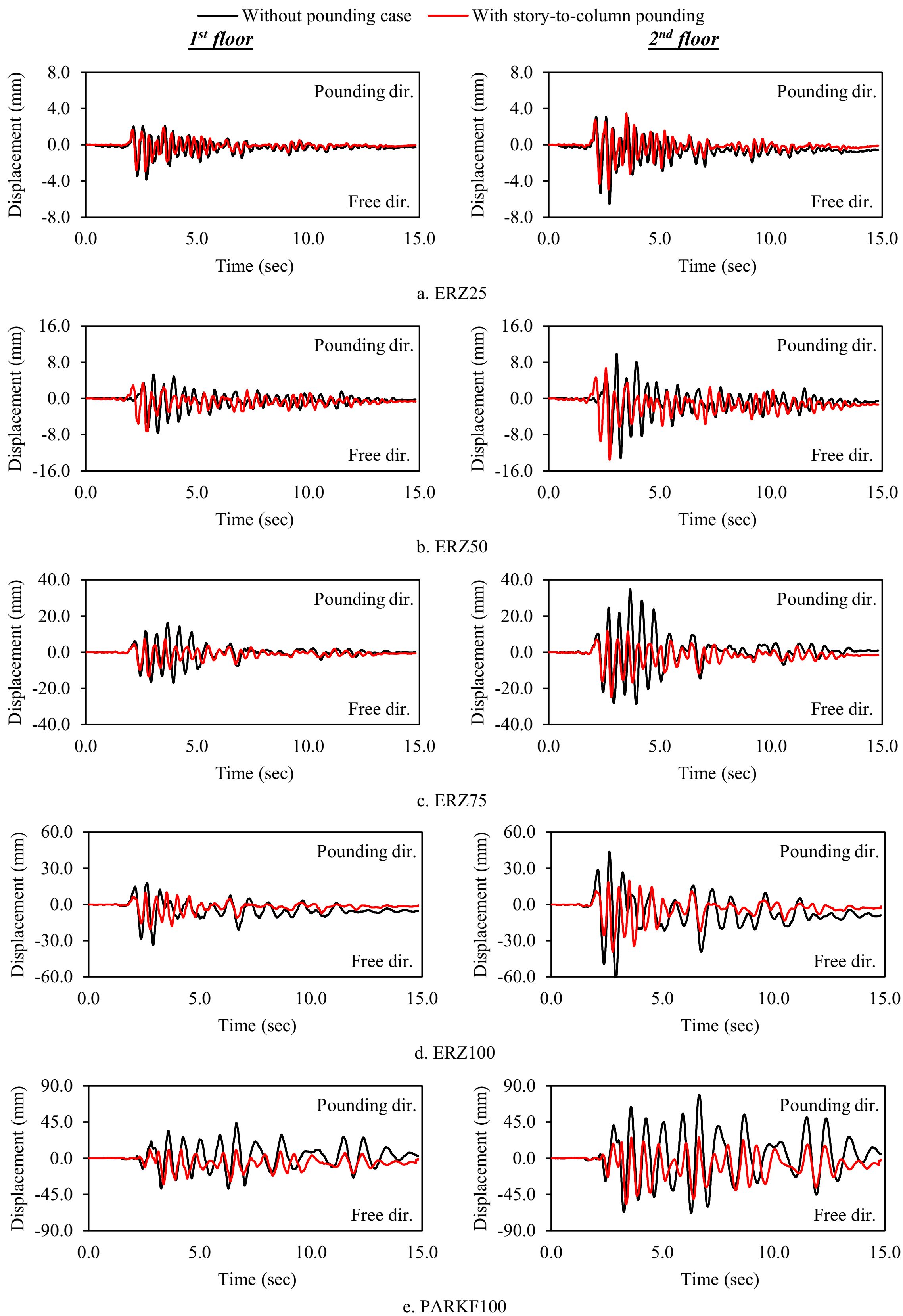

Figure 12. Changes in the time history of displacements due to pounding

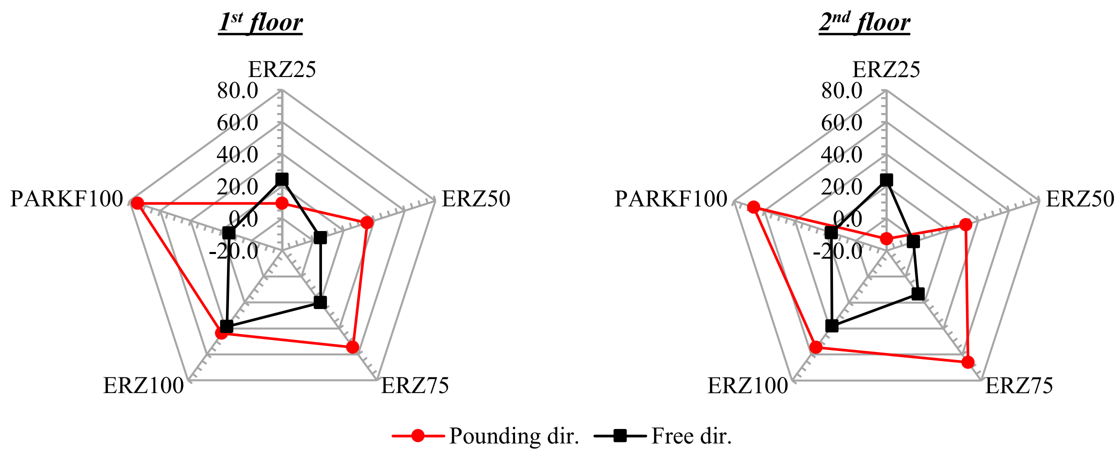

Figure 13. The story-to-column pounding-induced changes in maximum displacements

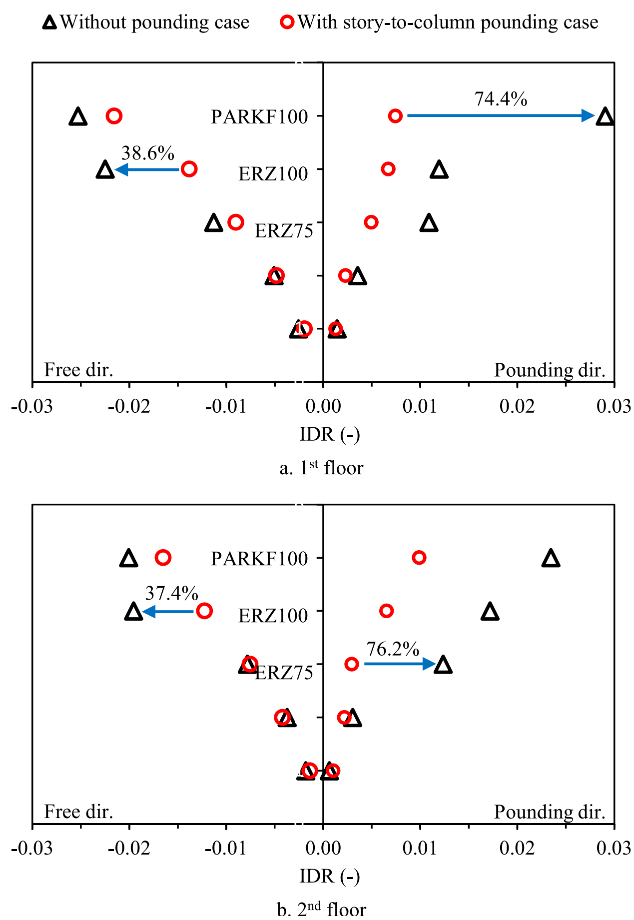

Figure 14. Changes in the IDRs due to pounding

without pounding case, the test specimen exhibited large displacements even at low lateral load level, as expected. However, in the test specimen subjected to pounding, the base shear forces increased abruptly due to interaction, while displacement responses decreased sharply. Consequently, the hysteresis loops became irregular and asymmetrical after the collisions. This asymmetry indicated that the pounding direction behaved differently due to repeated impacts, leading to varying energy distribution during each loading cycle.

3.4 Modal parameters

To investigate the effects of damage (visible or not) on structural behavior under increasing ground motion intensity, the modal parameters (frequencies, mode shapes, and damping ratios) of the RC test specimens were determined using AVTs. A total of 8 vibration tests were conducted for each test specimen. These are listed as follows:

- Condition 1: The first vibration test was conducted before the shake table experiments, with no additional masses placed on the undamaged test specimens.
- Condition 2: The second vibration test was conducted after additional masses were applied to the undamaged test specimens for the shake table experiments.
- Condition 3–7: The modal parameters of the specimens were identified following the shake table experiments conducted with increasing ground motion intensities.
- Condition 8: This represents the scenario where AVTs were conducted on the damaged test specimen without additional masses after the shake table experiments.

Vibration measurements were taken from a total of 16 different points of test specimens. These accelerometers were positioned at potential plastic hinge regions (0.5 h), in the middle of each column and at column-beam joints (Fig. 5). Enhanced frequency domain decomposition (EFDD) method was used to identify the modal parameters. Additional information about this method can be found in the literature [3, 28]. The processing of the dataset and identification was carried out using PULSE operational modal analysis [31]

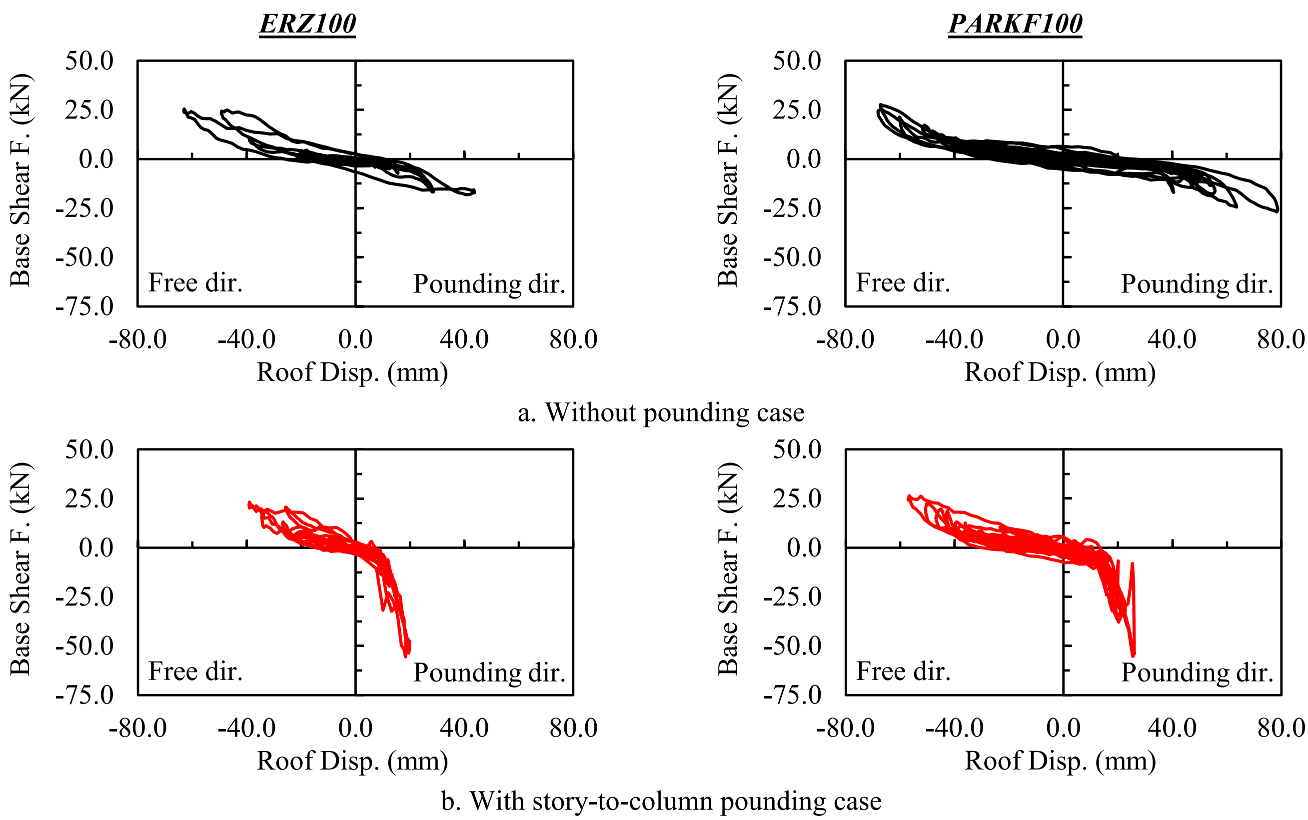

Figure 15. Comparison of hysteresis responses

software. The frequency range and duration were set as 0–100 Hz and 15 min, respectively. To minimize the leakage effects, a Hanning window was also used. Singular values of spectral density matrices (SVSDM) of the dataset obtained by the EFDD method are shown in Figs. 16 and 17 for both undamaged specimens with additional masses and damaged specimens after shake table tests. The variation of frequencies and damping ratios due to damage is a critical parameter for assessing the degradation of structural dynamic properties. The frequency and damping ratio values of both test specimens, which changed with increasing damage, are presented in Fig. 18. As the intensity of the ground motion applied on the shaking table increased, the frequency values decreased due to the damage that occurred. The reductions in the first two frequencies of the first test specimen (without pounding case), compared to the undamaged condition, were determined as follows: 5.97–6.41% for ERZ25, 12.08–13.50% for ERZ50, 22.58–24.97% for ERZ75, 29.97–33.37% for ERZ100, and 31.05–36.54% for PARKF100. In the test specimen where the pounding effects were considered, these values were determined as 6.73–7.34% for ERZ25, 11.78–13.18% for ERZ50, 20.20–21.10% for ERZ75, 26.89–30.03% for ERZ100, and 33.27–36.64% for PARKF100. On the other hand, damping ratios generally increased due to damage because energy dissipation mechanisms became more pronounced. However, Günaydin [15] emphasized that fluctuations in vibration signal amplitudes during AVTs could significantly impact the measured damping ratios, making it challenging to establish a direct link between changes in damping ratios and damage severity. In addition, Cao et al. [6] noted that, unlike natural frequencies and mode shapes, the effectiveness of damping as an indicator of damage requires further investigation and clarification.

Mode shapes are sensitive to structural damage, and it results in significant changes in mode shapes. These changes in mode shapes are often localized near the damaged region and can serve as indicators to evaluate the change in structural behavior. Figure 19 presents a comparison of the first two mode shapes of the test specimens identified before and after shake table tests. As can be clearly seen from Fig. 19, it was found that the mode shapes changed significantly with structural damage, and there was no agreement between the undamaged and damaged conditions. To better explain the effect of pounding on modal parameters, modal assurance criterion (MAC) values were calculated, and their reduction

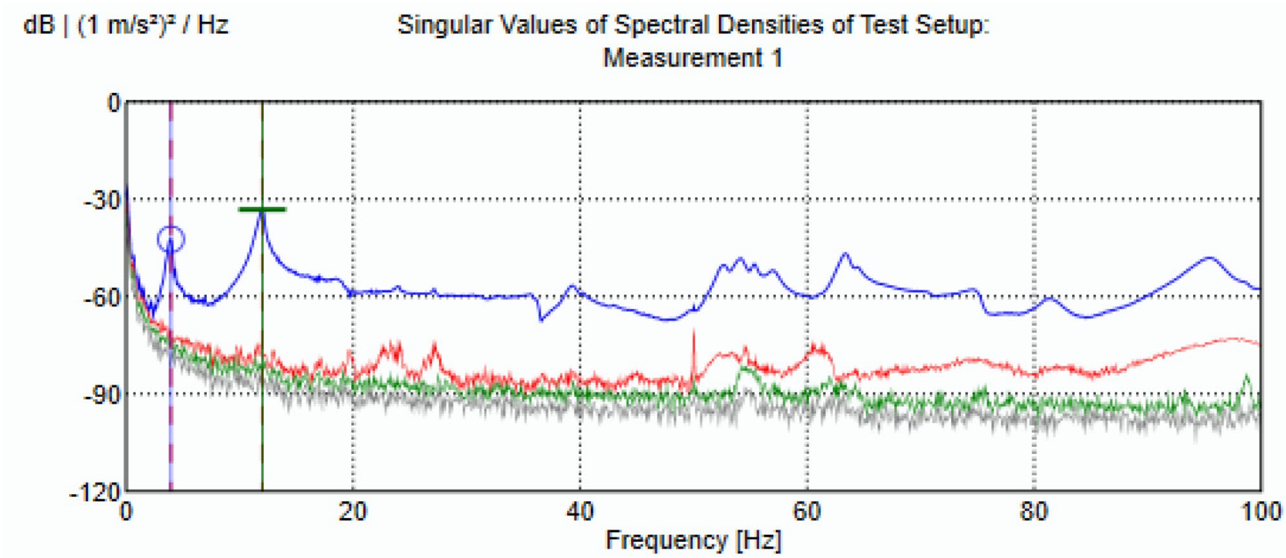

a. Undamaged state

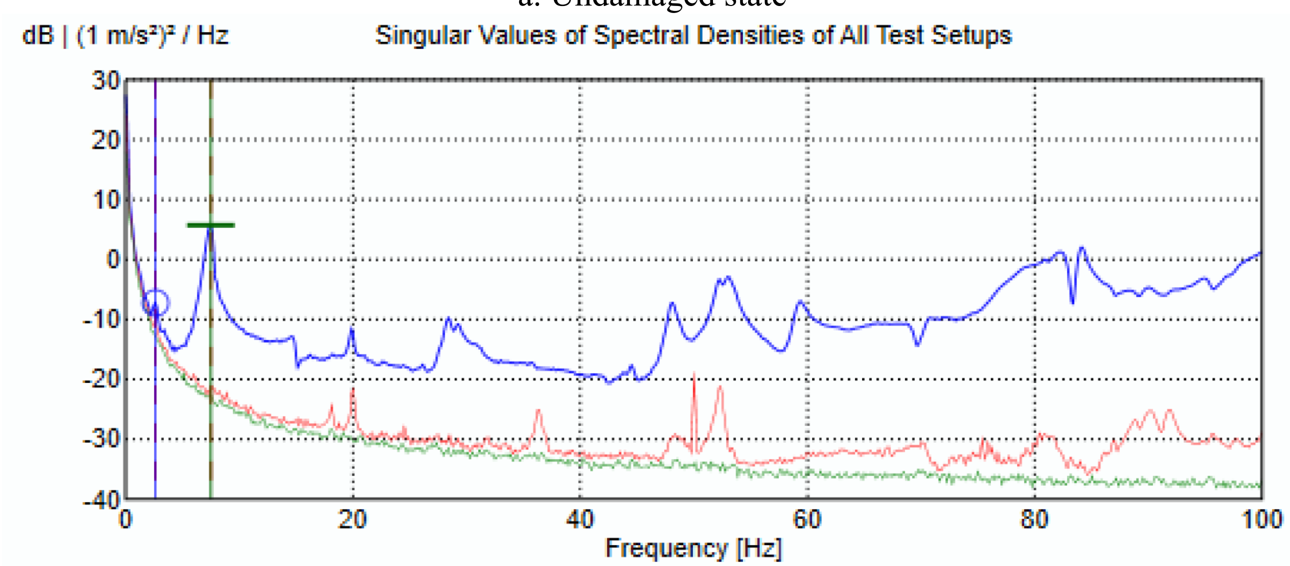

b. After shake table tests

Figure 16. SVSDM of data sets of the first test specimen (without pounding case)

with damage was examined (Fig. 20). The MAC compares the mode shape vectors obtained from the structure in undamaged and damaged conditions. A MAC value close to 1 indicates a high similarity between the mode shapes obtained under different conditions. Therefore, significant decreases in MAC values indicate the presence of damage. As observed in Fig. 20, the MAC values in the test specimen where the pounding effects were not considered significantly decreased after the PARKF100 earthquake due to damage. In contrast, in the test specimen with pounding effects considered the MAC values began to exhibit a significant decreasing trend with the ERZ75 records. This trend, as shown in Figs. 7 and 8, was attributed to shear damage in the columns caused by pounding. This clearly demonstrated that pounding effects, often overlooked in design, had significant impacts on modal parameters.

Figure 17. SVSDM of data sets of the second test specimen (with pounding case)

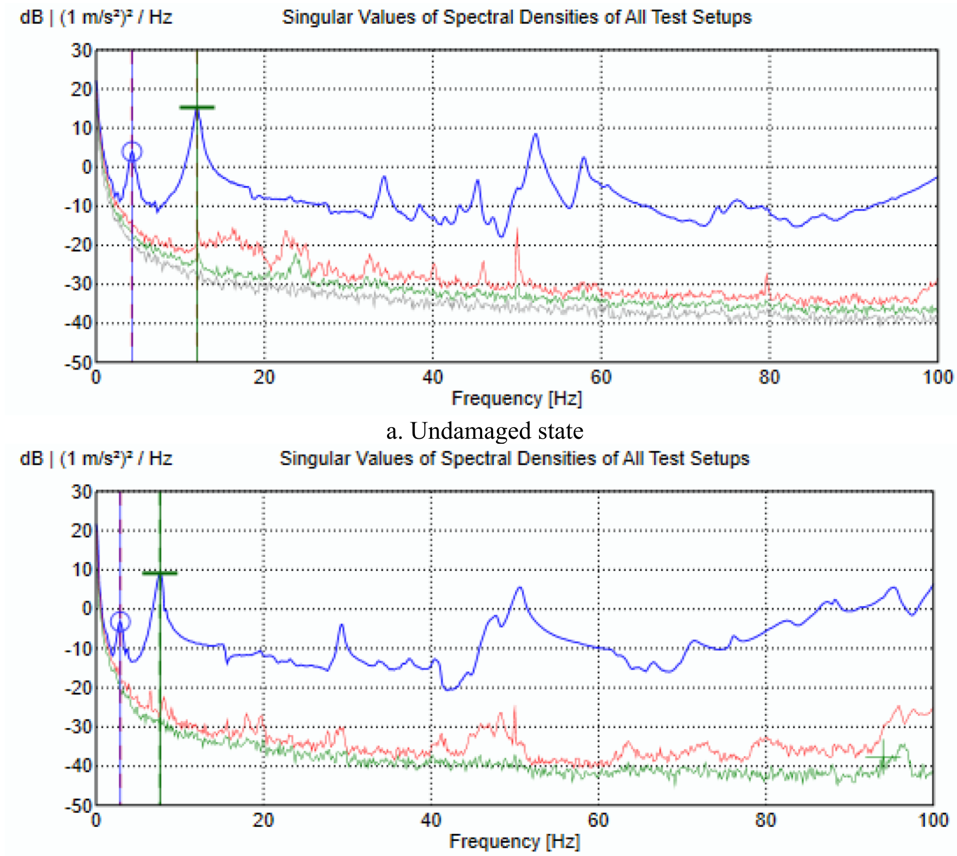

a. Undamaged state

b. After shake table tests

4 Conclusions

This study presents a large-scale experimental investigation of the effects of story-to-column pounding between adjacent RC buildings. Two half-scaled two-story RC frames were constructed in laboratory conditions and tested on a unidirectional shake table. In the tests, two scenarios were considered: (i) without pounding case and (ii) with story-to-column pounding case. This study aims to contribute to the literature by presenting one of the limited large-scale experimental investigations focusing on story-to-column pounding in RC buildings. Direct experimental comparisons were conducted between pounding and non-pounding scenarios under identical seismic inputs, and the collision-induced damage mechanisms were examined in detail through vibration testing. As a result of tests, the accelerations, displacements, IDRs, and modal parameters of the test specimens were thoroughly compared and analyzed in detail. Based on the experimental results, the following conclusions were drawn:

- Previous experimental studies have mostly focused on story-to-story pounding and few studies have been conducted on story-to-column pounding, which have more destructive effects. However, during the shake table tests, significant shear damage occurred in the column of the test specimen due to the interaction between the column and the story. No such localized shear damage was observed in without pounding case, confirming the destructive effect of direct story-to-column collisions.
- The sudden changes in velocity caused by pounding led to short-duration, high-amplitude spikes in floor accelerations. The pounding-induced increases in peak acceleration values obtained at the 1st and 2nd floors were calculated as 1.89–5.59% for the ERZ25, 25.12–58.23% for the ERZ50, 42.72–39.34% for the ERZ75, 66.82–105.14% for the ERZ100, and 43.57–135.57% for the PARKF100.
- The force–displacement behavior of the test specimen showed irregular and asymmetric hysteresis loops in the pounding case. These loops were characterized by sharp reversals and localized stiffness degradation, indicating varying energy distribution in the pounding direction due to repeated impacts. In contrast, the non-pounding case exhibited smoother and more symmetrical loops.

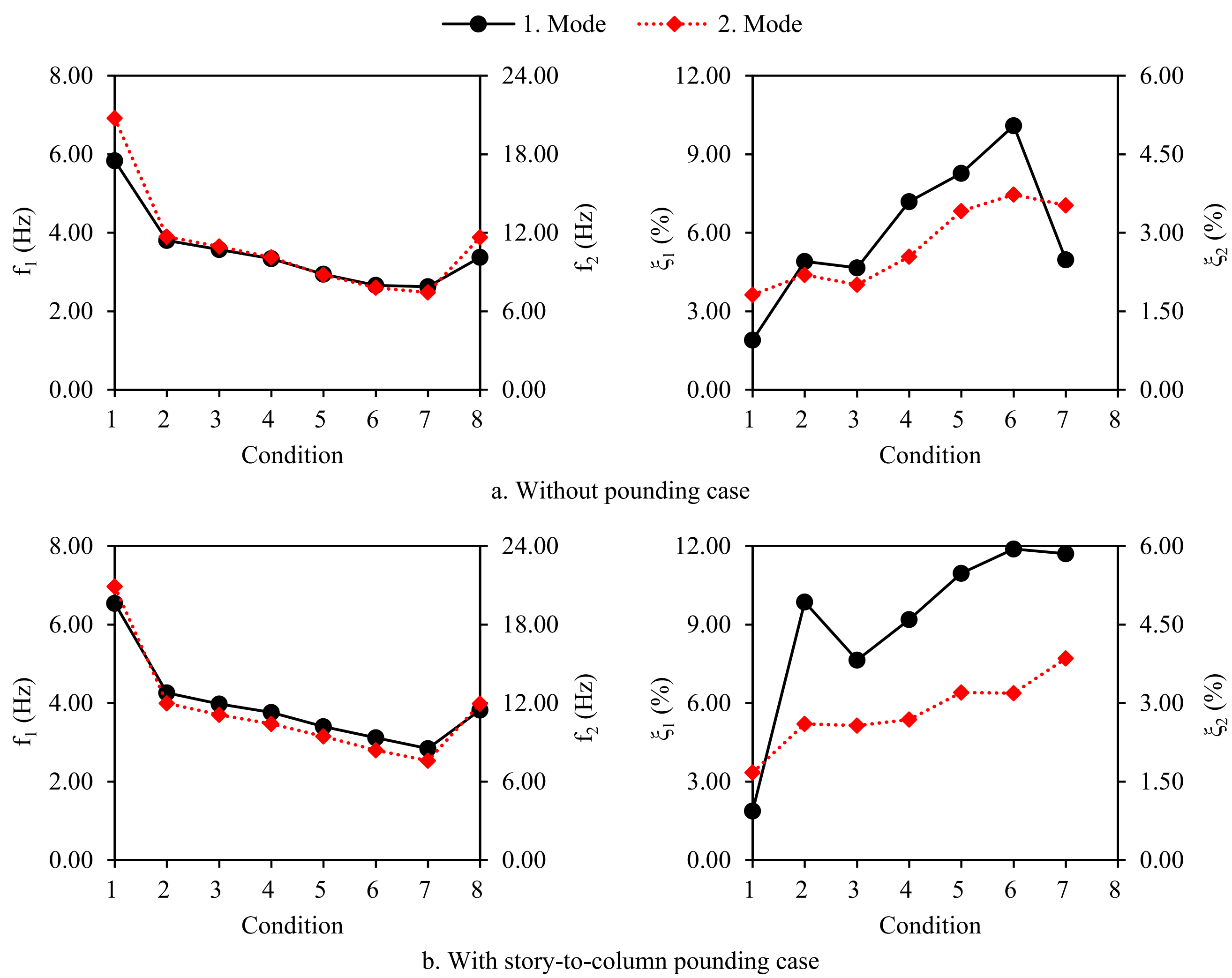

Figure 18. The variation of frequencies and damping ratios due to damage

- Pounding damages have mostly been studied observationally after past earthquakes. In this study, damages and the effects of collision on structural damages are investigated in detail by vibration tests. The experimental results demonstrated that pounding effects had a significant impact on modal parameters. While MAC values of the test specimen without pounding showed reductions after the PARKF100 earthquake, those with pounding effects exhibited declines starting from the ERZ75 records. These findings highlighted the importance of considering pounding effects in structural design to better predict changes in dynamic characteristics.

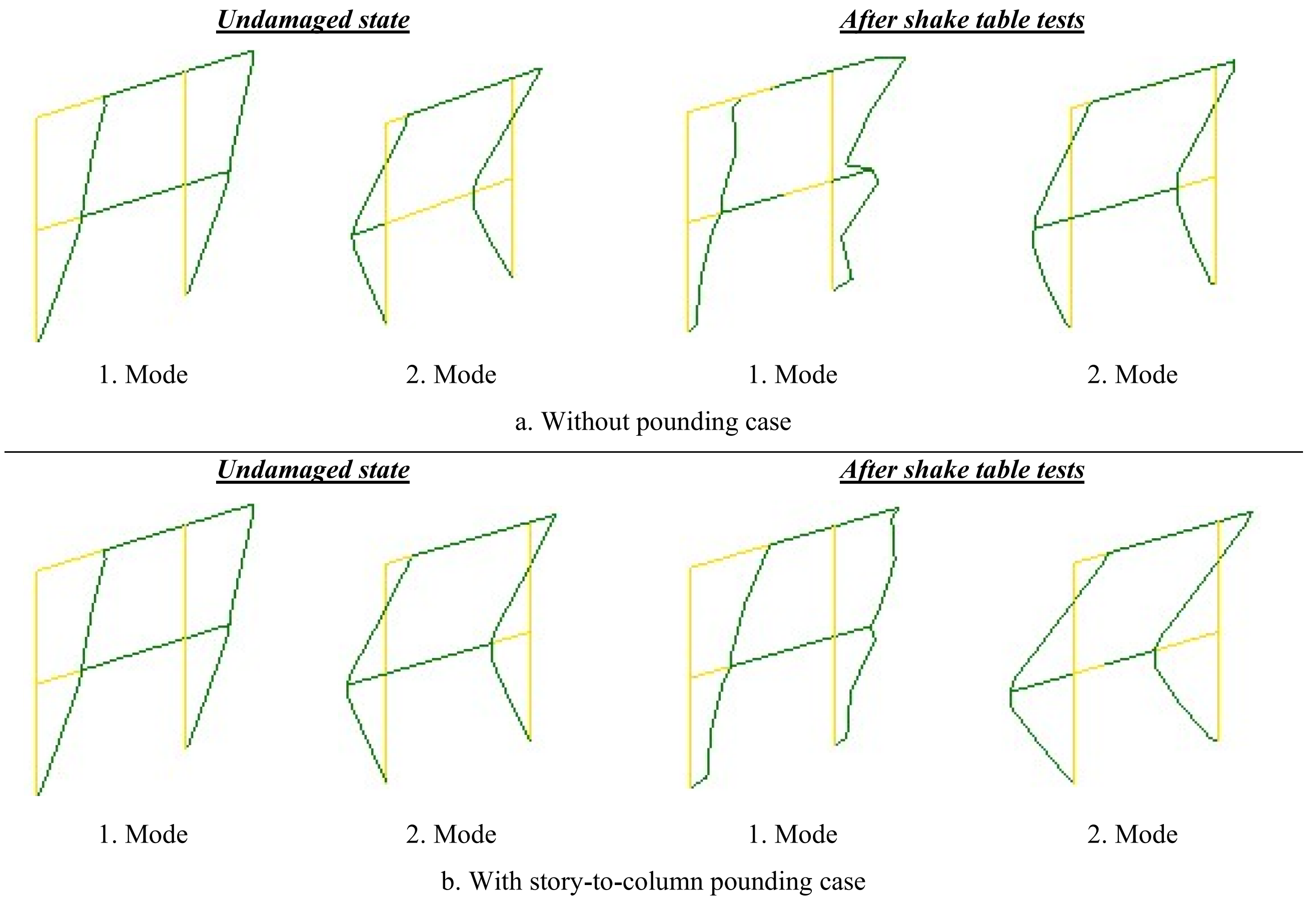

Figure 19. The changes in mode shapes of the test specimens due to damage

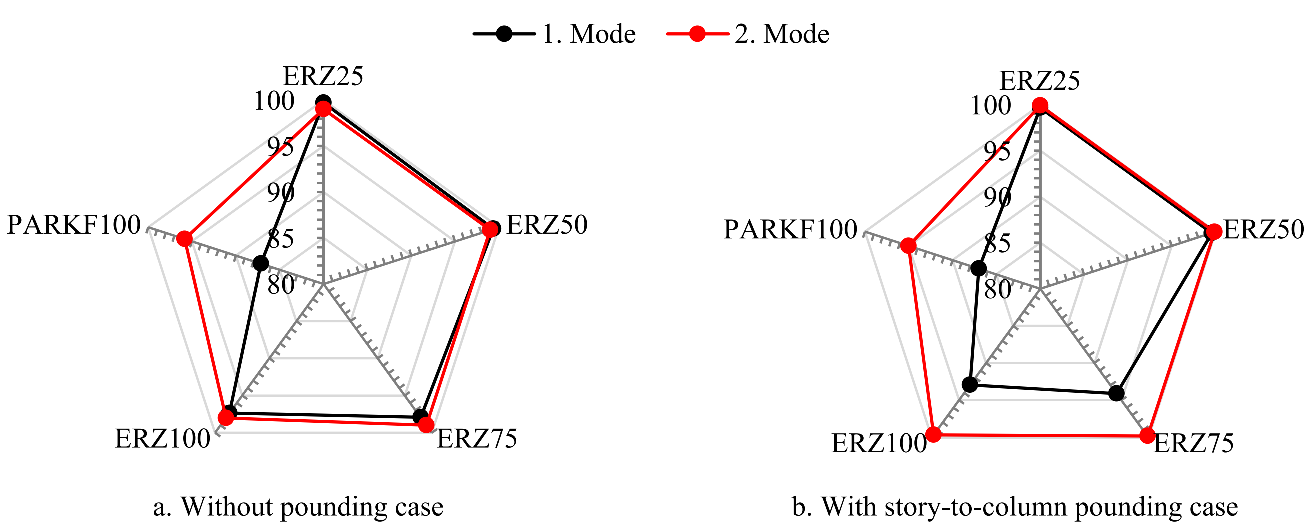

Figure 20. MAC values between the undamaged and damaged identified mode shapes

Acknowledgement This work was supported by the Scientific Research Projects Unit of Karadeniz Technical University (Project Numbers: FAY-2018–7715, FBA-2021–9227 and FBA-2021–9635).

Author contributions Ali Fuat GENÇ: validation, investigation, data curation. Muhammed Cihat ŞAHİN: investigation, formal analysis, data curation. Ahmet Can ALTUNISIK: writing—review and editing, supervision, resources, project administration, methodology, funding acquisition, conceptualization. Doğa ŞEN: validation, investigation, data curation. Ali KAYA: validation, investigation, data curation. Algıhan Kaşif KARAHASAN: investigation, formal analysis, Data curation. Fezayil SUNCA: writing—original draft, visualization, methodology, investigation, data curation, conceptualization.

Data availability Some or all data, models, or code that support the findings of this study are available from the corresponding author upon reasonable request.

Declarations

Competing interests We wish to confirm that there are no known conflicts of interest associated with this publication and there has been no significant financial support for this work that could have influenced its outcome.

References

1. Abdel Raheem SE, Fooly MY, Abdel Shafy AG, Taha AM, Abbas YA, Abdel Latif MM (2019) Numerical simulation of potential seismic pounding among adjacent buildings in series. Bull Earthquake Eng 17:439–471
2. Ahmad N, Shahzad A, Rizwan M, Khan AN, Ali SM, Ashraf M, Naseer A, Ali Q, Alam B (2019) Seismic performance assessment of non-compliant SMRF-reinforced concrete frame: shake-table test study. J Earthq Eng 23(3):444–462
3. Altunışık AC, Bayraktar A, Sevim B, Ateş Ş (2011) Ambient vibration based seismic evaluation of isolated Gülburnu highway bridge. Soil Dyn Earthq Eng 31(11):1496–1510
4. Altunışık AC, Arslan ME, Kahya V, Aslan B, Sezdirmez T, Dok G, Nas M (2023) Field observations and damage evaluation in reinforced concrete buildings after the february 6th, 2023, Kahramanmaras-Turkiye Earthquakes. J Earthq Tsunami
5. Anagnostopoulos SA (1996) Building pounding re-examined: how serious a problem is it. In: Eleventh World conference on earthquake engineering. Oxford, UK
6. Cao MS, Sha GG, Gao YF, Ostachowicz W (2017) Structural damage identification using damping: a compendium of uses and features. Smart Mater Struct 26(4):043001
7. Cayci BT, Akpinar M (2021) Seismic pounding effects on typical building structures considering soil-structure interaction. Structures 34:1858–1871
8. Chau KT, Wei XX, Guo X, Shen CY (2003) Experimental and theoretical simulations of seismic poundings between two adjacent structures. Earthq Eng Struct Dyn 32(4):537–554
9. Chau KT, Wei XX, Shen CY, Wang LX (2004) Experimental and theoretical simulations of seismic torsional poundings between two adjacent structures. In: 13th World conference on earthquake engineering, Vancouver, Canada
10. Chau KT, Wang LX, Wei XX (2006) Torsional poundings between two adjacent asymmetric structures. In: 4th International conference on earthquake engineering, pp 12–13
11. Crozet V, Politopoulos I, Chaudat T (2019) Shake table tests of structures subject to pounding. Earthq Eng Struct Dyn 48(10):1156–1173
12. Efraimiadou S, Hatzigeorgiou GD, Beskos DE (2013) Structural pounding between adjacent buildings subjected to strong ground motions. Part I: the effect of different structures arrangement. Earthq Eng Struct Dyn 42(10):1509–1528
13. El-Khoriby S, Seleemah A, Elwardany H, Jankowski R (2015) Experimental and numerical study on pounding of structures in series. Adv Struct Eng 2:1073–1089
14. Filiatrault A, Wagner P, Cherry S (1995) Analytical prediction of experimental building pounding. Earthq Eng Struct Dyn 24(8):1131–1154
15. Günaydin M (2016) Investigation of dynamic behavior of repaired and strengthened reinforced concrete buildings using fiber reinforced polymer composite materials with experimental and analytical methods. Ph.D. dissertation (in Turkish), Karadeniz Technical University, Trabzon
16. Jankowski R, Seleemah A, El-Khoriby S, Elwardany H (2015) Experimental study on pounding between structures during damaging earthquakes. Key Eng Mater 627:249–252
17. Jiang S, Zhai C, Liu Y (2022) Experimental and numerical studies of seismic induced story-to-story and inter-story pounding. Structures 46:555–569
18. Kamal M, Inel M, Cayci BT (2022) Seismic behavior of mid-rise reinforced concrete adjacent buildings considering soil-structure interaction. J Build Eng 51:104296
19. Karayannis CG, Naoum MC (2018) Torsional behavior of multistory RC frame structures due to asymmetric seismic interaction. Eng Struct 163:93–111
20. Kasai K, Maison BF (1997) Building pounding damage during the 1989 Loma Prieta earthquake. Eng Struct 19(3):195–207
21. Khan FA, Khan SW, Rashid M, Rizwan M, Fahim M, Shahzada K, Ahmad N, Badrashi YI, Qazi S, Said I (2021) Evaluation of code compliant/non-compliant ECC-RC IMRF structures. Structures 32:1634–1645
22. Kharazian A, López Almansa F, Benavent Climent A, Gallego Molina A (2018) Shaking table testing on seismic pounding of a RC building structure. In: Proceedings of the DINEST 2018. Spain
23. Khatiwada S, Chouw N (2013) A shake table investigation on interaction between buildings in a row. Coupled Syst Mech 2(2):175–190
24. Kazemi F, Miari M, Jankowski R (2021) Investigating the effects of structural pounding on the seismic performance of adjacent RC and steel MRFs. Bull Earthq Eng 19(1):317–343
25. Manoukas GE, Karayannis CG (2023) Seismic interaction between multistory pilotis RC frames and shorter structures with different story levels—floor-to-column pounding. CivilEng 4(2):618–637
26. Miari M, Jankowski R (2022) Shaking table experimental study on pounding between adjacent structures founded on different soil types. Structures 44:851–879
27. Miglietta M, Damiani N, Guerrini G, Graziotti F (2021) Full-scale shake-table tests on two unreinforced masonry cavity-wall buildings: effect of an innovative timber retrofit. Bull Earthq Eng 19:2561–2596
28. Nasery MM, Hüsem M, Okur FY, Altunışık AC (2020) Damage effect on experimental modal parameters of haunch strengthened concrete-encased composite column–beam connections. Int J Damage Mech 29(2):297–334
29. Papadrakakis M, Mouzakis HP (1995) Earthquake simulator testing of pounding between adjacent buildings. Earthq Eng Struct Dyn 24(6):811–834
30. PEER (2021) Pacific earthquake engineering research center, University of California, Berkeley
31. PULSE (2021) PULSE operational modal analysis, release 7.1. Structural Vibration Solution A/S, Denmark
32. Quintana-Gallo P, Pampanin S, Carr AJ, Bonelli P (2010) Shake table tests of under-designed RC frames for the seismic retrofit of buildings–design and similitude requirements of the benchmark specimen. Proceedings of the New Zealand Society of Earthquake Engineering

33. Rezavandi A, Moghadam AS (2007) Experimental and numerical study on pounding effects and mitigation techniques for adjacent structures. Adv Struct Eng 10(2):121–134
34. Romão X, Costa AA, Paupério E, Rodrigues H, Vicente R, Varum H, Costa A (2013) Field observations and interpretation of the structural performance of constructions after the 11 May 2011 Lorca earthquake. Eng Fail Anal 34:670–692
35. Rosenblueth E, Meli R (1986) The 1985 Mexico earthquake. Concr Int 8(5):23–34
36. Salem YS, Feng M (2008) Shake testing of frame structures retrofitted with viscous dampers to mitigate seismic pounding. In: 14th World conference on earthquake engineering, Beijing, China
37. Shrestha B, Hao H (2018) Building pounding damages observed during the 2015 Gorkha earthquake. J Perform Constr Facil 32(2):04018006
38. Sołtysik B, Falborski T, Jankowski R (2017) Preventing of earthquake-induced pounding between steel structures by using polymer elements–experimental study. Procedia Eng 199:278–283
39. Sunca F, Altunişik AC, Kaya A, Genç AF, Şahi̇n MC, Karahasan AK (2024) Shake table tests on story-to-story pounding between adjacent RC buildings. Structures 69:107544
40. Takabatake H, Yasui M, Nakagawa Y, Kishida A (2014) Relaxation method for pounding action between adjacent buildings at expansion joint. Earthq Eng Struct Dyn 43(9):1381–1400
41. Wu QY, He WC, Wei M, Zhu HP (2019) Theoretical and experimental study on critical separation distance of adjacent buildings based on seismic pounding fragility. J Eng Mech 145(12):04019106
42. Zhang H, Kuang JS, Yuen TY (2017) Low-seismic damage strategies for infilled RC frames: shake-table tests. Earthq Eng Struct Dyn 46(14):2419–2438